Mu-Mesonic X-Rays and the Shape of the Nuclear Charge Distribution

DAVID L. HILL,* *University of California, Los Alamos Scientific Laboratory, Los Alamos, New Mexico*

AND

KENNETH W. FORD, *Indiana University,† Bloomington, Indiana*

(Received March 8, 1954)

Mu-mesonic x-rays, fast electron scattering, and electronic spectra each depend on the nuclear charge distribution $\rho(r)$ in different ways. Adjoining theoretical analyses of observations on these different phenomena may therefore bracket an acceptable set of functional descriptions for $\rho(r)$. The present paper reports the dependence of the μ-mesonic x-ray spectrum of Pb on the extent and shape of the nuclear charge density. For several functional families representing conceivable forms for $\rho(r)$ we have obtained the resultant Coulomb potentials and have solved "exactly" by electronic computation the relativistic equations to yield the first four levels ($1S$, $2S$, and $2P$) and transition energies for mu mesons bound in the field of the lead nucleus. The next two levels ($3D$) have been found by perturbation theory. Effects omitted from the calculations have been examined and theoretical uncertainties estimated for each level. These results permit adjustment of the effective electric radius R, for each form of $\rho(r)$ to agree with known x-ray measurements of the $2P\rightarrow 1S$ transitions. Calculations completed for neighboring values of R permit interpolation to improved values when more precise measurements are made and when small corrections of the raw data for electrodynamic and special coupling effects have been carried through. The doublet splitting of the $2P$ levels offers an independent measure of R, as well as a check on the possible existence of an anomalous muon magnetic moment. In contrast, the $3D\rightarrow 2P$ and $2S\rightarrow 2P$ transition energies are insensitivie to R but sufficiently sensitive to the shape of the charge distribution, so that accurate measurements of the transition energies between the six lowest muon levels in the heavy nuclides will be able to provide information on both the electrical radius and the shape of nuclear electrification, independently of indications from the other phenomena mentioned above.

I. INTRODUCTION

A NUMBER of sources of evidence now give a strong indication that the electromagnetic radii of heavy nuclei are at least 15 percent smaller than the previously assumed values of $(1.4 \text{ to } 1.5)\times 10^{-13}A^{1/3}$ cm.[1] The only contrary evidence comes from the study by Schawlow and Townes[2] of the effect of the finite size of the nucleus on the electronic x-ray fine structure. The disagreement between this and other sources of evidence has not been explained, but may be due to radiative corrections to the $p_{1/2}$ electronic level. In view of the rather convincing evidence for the smaller *size* of the nuclear proton distribution, it is of interest to know whether the charge distribution is also altered in shape from our previous ideas of a nearly uniform density. (By shape we here mean the shape of the curve of nuclear proton density *vs* radius, and not the geometric shape of the nucleus.) In the present paper we show that the mu-mesonic x-ray transitions can provide a valuable tool in the determination of the shape of the charge distribution within the nucleus[3]—both alone and in conjunction with other sources of evidence.

Among known experimental results which depend on the charge distribution in the nucleus, the $2P\rightarrow 1S$ mu-mesonic transition energy[4] probably provides most unambiguously a single parameter of the charge distribution.[5] If this transition energy is the most reliable single datum that we have on the nuclear charge distribution, it can reasonably be used to delimit somewhat the set of all possible charge distributions. For example, for any assumed *shape* of distribution, the mu-mesonic transition energy can be used as a constraint to yield a radial extent, or *range* of the distribution. Other effects can then be investigated using this limited set of charge distributions.

In the present paper, we generate a set of charge distributions for the Pb nucleus more or less covering the range of reasonable shapes, limited by the requirement that for each the $2P_{3/2}\rightarrow 1S$ transition energy for the mu meson is 6.00 Mev. In order to allow for future corrections to the measured transition energy, to the mu-meson mass, or to the theoretical interpretation, we evaluate the lowest mu-meson levels in fact for each assumed shape at several ranges in the vicinity of the range which yields the transition energy of 6 Mev.

In practice, a two or three parameter family of charge distributions can rather thoroughly cover the field of reasonable possibilities. Hence, the mu-mesonic $2P\rightarrow 1S$ datum (for Pb, say) can reduce the set to a one or two parameter family. Other effects, which also depend on the nuclear charge distribution, but in a different way, can then be considered to delimit the field further and in principle to give a rather complete picture of the charge distribution. Some of these effects, which have received previous theoretical treatment, or which do not require detailed calculations, are considered in the

* On leave from Vanderbilt University, Nashville, Tennessee.

† Joint program of the U. S. Office of Naval Research and the U. S. Atomic Energy Commission.

[1] F. Bitter and H. Feshbach, Phys. Rev. **92**, 837 (1953).

[2] A. L. Schawlow and C. H. Townes, Science **115**, 284 (1952).

[3] J. A. Wheeler, Revs. Modern Phys. **21**, 133 (1949); Phys. Rev. **92**, 812 (1953).

[4] V. L. Fitch and J. Rainwater, Phys. Rev. **92**, 789 (1953).

[5] L. N. Cooper and E. M. Henley, Phys. Rev. **92**, 801 (1953).

succeeding paper.[6] It is shown that in fact in the present state of our knowledge they cast very little additional light on the question of the shape of the charge distribution.

Effects, which at present require exact numerical calculation, are

A. $3D \rightarrow 2P$ and $2S \rightarrow 2P$ mu-mesonic transitions.[3]
B. Very high energy electron scattering.[7-9]

The first of these we consider in the present paper. The second contains in principle a great deal of information and has received considerable attention already.[7-9] The freedom of choice of nuclear radius, however, has led to a great freedom in shapes[10] of charge distributions which can fit the data.[9] A principal utility of the present calculations may be providing a constraint on the radius for each shape of charge distribution and thereby in narrowing the field of shapes which can fit the electron scattering data. Detailed calculations of the electron scattering with the mu-meson-restricted charge distributions are now in progress.

Specifically, the results of the present calculations are values of the binding energy of the negative mu-meson in the lowest four states ($1S$, $2P_{1/2}$, $2P_{3/2}$, $2S$) in the field of the Pb nucleus, for a variety of assumed shapes of the nuclear charge distribution, and for a number of radii (or ranges) for each shape. The mu-mesonic wave functions are also obtained. The energies of the next two states ($3D_{3/2}$, $3D_{5/2}$) are obtained for the exponential distribution by perturbation theory, and are scaled to other shapes and sizes of charge distribution with an accuracy of about 1 kev. The main features of the pattern which emerges are the following: (1) The radius of a uniform charge distribution yielding a $2P_{3/2} \rightarrow 1S$ transition energy of 6.00 Mev is 6.94×10^{-13} cm$=1.17 \times 10^{-13}\ A^{1/3}$ cm, in agreement with Fitch and Rainwater[4] and Cooper and Henley.[5] The decay length of an exponential charge distribution yielding the same transition energy is 1.78×10^{-13} cm$=0.300 \times 10^{-13}\ A^{1/3}$ cm. (2) The rate of variation of transition energies with nuclear size is very different for different transitions, and is summarized in Table I. (3) The absolute values of the meson binding energies are very insensitive to change of shape of the nuclear charge distribution for fixed $2P_{3/2} \rightarrow 1S$ transition energy. (4) The $3D \rightarrow 2S$ and $2S \rightarrow 2P$ transitions are more sensitive to shape of charge distribution than to nuclear size and could be utilized to advantage to yield an indication of the shape of the nuclear charge distribution. For fixed $2P_{3/2} \rightarrow 1S$ transition energy, the $3D \rightarrow 2P$ energies vary by about 5 percent and the $2S \rightarrow 2P$ energies by about 15 percent between the uniform and exponential charge distributions. (5) The $2P$ doublet splitting is sensitive to nuclear size, and therefore provides an independent check on the nuclear radius (or a way to check for the existence of an anomalous magnetic moment of the muon). For $2P_{3/2} \rightarrow 1S$ energy$=6.00$ Mev, the fine structure splitting is predicted to be 176 kev for the exponential charge distribution, 186 kev for the uniform charge distribution, and to lie between these figures for all other calculated distributions.

[6] K. W. Ford and D. L. Hill, succeeding paper [Phys. Rev. **94**, 1630 (1954)].
[7] Hofstadter, Fechter, and McIntyre, Phys. Rev. **92**, 978 (1953).
[8] L. I. Schiff, Phys. Rev. **92**, 988 (1953).
[9] Yennie, Wilson, and Ravenhall, Phys. Rev. **92**, 1325 (1953).
[10] More recent analysis [R. Hofstadter, Phys. Rev. **94**, 773 (T) (1954)] gives evidence of a charge distribution not greatly different from uniform.

II. QUALITATIVE DESCRIPTION AND ESTIMATED PERTURBATIONS

In a first-order perturbation approximation, in which Dirac wave functions are used, the finite extension of the nucleus raises the mu-mesonic $1S$ state energy above its point-nucleus value by an amount proportional to

$$\langle r^{2\sigma} \rangle_{\text{Av}} \equiv \frac{4\pi}{Ze} \int \rho(r) r^{2\sigma+2} dr,$$

where $\rho(r)$ is the nuclear charge density, and

$$\sigma = [1-(\alpha Z)^2]^{1/2},$$

Z being the nuclear charge and $\alpha = 137.038^{-1}$ being the fine structure constant. The $2S$ and higher S-state energies are raised, in proportion to the same integral with successively smaller coefficients. The $2P_{1/2}$ energy is raised, in proportion to the same integral, with coefficient small compared to that for the $2S$ state; the $2P_{3/2}$ energy is unchanged (to first order). Hence, for light nuclei, where the perturbation approximation is valid (and for which $\sigma \cong 1$), all of the properties of the mu-mesonic x-ray spectrum are determined by the value of $\langle r^2 \rangle_{\text{Av}}$, the mean square radius integrated over the nuclear charge distribution.[1,3,5]

For heavy nuclei, the effect of the finite size of the nucleus on the mu-mesonic levels is large and exact

TABLE I. Sensitivity of energies to nulcear size. The numbers, a_i, in the table are percent changes in energies for a 1 percent increase in the radial parameter of the charge distribution in the vicinity of the "true" radius; i.e., $a_i = [(\gamma/E)(dE/d\gamma)]_i$.

Energy	Uniform distribution	Exponential distribution
$1S$	−0.514	−0.492
$2S$	−0.297	−0.268
$2P_{1/2}$	−0.158	−0.185
$2P_{3/2}$	−0.112	−0.144
$3D_{3/2}$	−0.006	−0.027
$3D_{5/2}$	−0.002	−0.011
$2P_{1/2} \rightarrow 1S$	−0.81	−0.74
$2P_{3/2} \rightarrow 1S$	−0.82	−0.75
$2S \rightarrow 2P_{1/2}$	+0.25	+0.10
$2S \rightarrow 2P_{3/2}$	+0.54	+0.36
$3D_{5/2} \rightarrow 2P_{3/2}$	−0.21	−0.26
$3D_{3/2} \rightarrow 2P_{3/2}$	−0.21	−0.25
$3D_{3/2} \rightarrow 2P_{1/2}$	−0.29	−0.32
Δ_P	−1.3	−1.3
Δ_D	−0.2	−1.0

calculation is required (Part III). The transition energy becomes relatively less sensitive to the extent of the charge distribution. We find for Pb that the shift of the $1S$ state energy from the point nucleus value varies approximately as $\langle r^{0.5}\rangle_{Av}$ rather than $\langle r^{2\sigma}\rangle_{Av}\equiv\langle r^{1.6}\rangle_{Av}$.

Possible uncertainties in the theoretical interpretation of the transition energies, most of which have already been considered by others, are here summarized, with comments. Quantitative estimates of the effects of these various perturbations on the calculated energies are summarized in Table III.

(a) *A nonelectromagnetic meson-nucleon interaction.* There is evidence that this interaction has approximately the same strength as the electron-nucleon beta decay interaction.[11] If so, it shifts the energy levels by less than 1 ev and is completely negligible.[5]

(b) *Anomalous magnetic moment of mu meson.* The electrodynamic contribution to the anomalous moment should have the same small relative value as for the electron ($\alpha/2\pi$), and increase the calculated $2P$ doublet splitting by less than 1 kev, a negligible effect. The nucleonic (pion field) contribution should be even much smaller because of the very small muon-nucleon interaction. If a sizable anomaly exists, however, only the $2P$ fine structure splitting would be appreciably affected.[3] It would of course be of great interest to look for such an effect.

(c) *Vacuum polarization—the Uehling effect.* As pointed out by Cooper and Henley[5] and by Corben,[12] the polarization of the vacuum by electron pairs produces an appreciable shift in the calculated, mu-mesonic energy levels. Because, for the levels calculated, the meson lies well within the distance of an electron Compton wavelength from the nucleus, it is a good approximation to use the limiting form of the vacuum polarization potential given by Schwinger[13] for $r\ll\lambda\!\!\!^{-}_c$. For a heavy nucleus this perturbing potential is, to first order in αZ,

$$V_p(r)=(2\alpha/3\pi)V_0(r)[\bar{l}(r)-(5/6)], \tag{1}$$

where $V_0(r)$ is the unperturbed electrostatic potential

$$V_0(r)=\int|\mathbf{r}-\mathbf{r}'|^{-1}\rho(\mathbf{r}')d(\mathrm{vol}'); \tag{2}$$

$\bar{l}(r)$ is defined by

$$\bar{l}(r)=\frac{1}{V_0(r)}\int\log\left(\gamma\frac{|\mathbf{r}-\mathbf{r}'|}{\lambda\!\!\!^{-}_c}\right)\frac{\rho(\mathbf{r}')}{|\mathbf{r}-\mathbf{r}'|}d(\mathrm{vol}');$$

$\lambda\!\!\!^{-}_c$ is the reduced electron Compton wavelength; and $\gamma=1.781$. The quantity $\bar{l}(r)$ is slowly varying over the region occupied by the mu meson, and we make the simplifying assumption of replacing $\bar{l}(r)$ by a constant.

[11] E. Amaldi and G. Fidecaro, Phys. Rev. **81**, 339 (1951); J. M. Kennedy, Phys. Rev. **87**, 953 (1952).
[12] H. C. Corben, Phys. Rev. **94**, 787(A) (1954).
[13] J. Schwinger, Phys. Rev. **75**, 651 (1949).

TABLE II. Factors in the polarization energy shift, Eq. (4). The coefficient C is equal to an approximate mean value of the quantity $(2\alpha/3\pi)[\bar{l}(r)-5/6]$. The average potential energy, $\langle V_0\rangle$, was calculated for the two distributions with $2P_{3/2}\rightarrow 1S$ energy = 6.00 Mev.

Level	C	Uniform $\langle V_0\rangle$	Exponential $\langle V_0\rangle$
$1S$	0.00404	−15.63 Mev	−15.68 Mev
$2S$	0.00297	−6.27	−6.42
$2P_{1/2}$	0.00356	−9.25	−8.85
$2P_{3/2}$	0.00346	−8.76	−8.41
$3D_{3/2}$	0.002(0)	−4.6	−4.6
$3D_{5/2}$	0.002(0)	−4.3	−4.3

For $r\ll R$ (the nuclear radius), and with the assumption of a uniform charge density, $\bar{l}(r)\cong\log(\lambda\!\!\!^{-}_c/\gamma R)+\frac{1}{2}$. For $r\gg R$, $\bar{l}(r)\cong\log(\lambda\!\!\!^{-}_c/\gamma r)$. We choose as an appropriate mean value for the $1S$ state, $\bar{l}=\log(\lambda\!\!\!^{-}_c/\gamma R)=3.44$, and for the $2S$ and $2P$ states smaller numbers, 2.75 and 3.10, respectively. For the $3D$ states, $\bar{l}$ is taken crudely to be 2.1. Then the energy shift due to the vacuum polarization is

$$\Delta E_p=C\langle V_0\rangle. \tag{4}$$

Values of the coefficients C and of the mean values of the potentials, $\langle V_0\rangle$, for the exponential and for the uniform distribution, are given in Table II. The energy shifts ΔE_p are included in Table III, and are estimated to be accurate to within 5 percent for the S and P states, 15 percent for the D states [the principal uncertainty arising in the choice of $\bar{l}(r)$]. This error does not include the uncertainty in the magnitude of higher order corrections, which have been ignored. Since αZ is not small compared to 1, higher order radiative effects may be appreciable. They have, however, been assumed negligible in Table III.

(d) *Other radiative effects.* Electrodynamic effects other than vacuum polarization by electrons arise from the coupling of the meson to the radiation field, and are consequently very much smaller in magnitude than the Uehling effect. Since the meson reduced Compton wavelength is substantially smaller than the radii of the meson orbits considered, a crude but presently adequate estimate for the other radiative effects (including the effect of the anomalous moment) can be made by utilizing the same approximations employed for the Lamb shift in hydrogen. One thereby obtains an estimated shift of order 1 kev for the $1S$ state and somewhat less for the $2S$ and $2P$ states.

(e) *Nuclear polarization effect.* The nuclear polarization effect has been estimated crudely by Cooper and Henley[5] for the $1S$ state by using closure over both nuclear and meson states with an average energy denominator of 20 Mev. Their result is $\Delta E=-60$ kev. Laking and Kohn[14] report an estimate of -16 ± 8 kev for the same effect. We have not attempted to improve on these estimates and include in Table III what is

[14] W. Lakin and W. Kohn, Phys. Rev. **94**, 787 (1954).

TABLE III. Summary of perturbations to calculated mu-mesonic energies. Those perturbations are included whose effect is estimated to be greater than 1 kev. Indicated uncertainties are, in all cases, intended to be upper limits to the error, rather than probable errors.

Effect	Estimated energy shifts in kev							
	$1S$	$2S$	$2P_{1/2}$	$2P_{3/2}$	$3D$	$2P\rightarrow 1S$	$2S\rightarrow 2P$	$3D\rightarrow 2P$
1. Vacuum polarization	-63 ± 5	-19 ± 2	-32 ± 3	-30 ± 3	-9 ± 3	$+32\pm8$	$+12\pm5$	$+22\pm5$
2. Other radiative effects	2 ± 2	0 ± 1	-0.6 ± 0.5	0.3 ± 0.5	···	-2 ± 3	0 ± 2	0 ± 1
3. Nuclear polarization	-50 ± 40	-8 ± 8	-7 ± 7	-4 ± 4	···	$+45\pm40$	-5 ± 10	$+5\pm5$
4. Mass of muon	0 ± 25	0 ± 12	0 ± 20	0 ± 20	0 ± 10	0 ± 5	0 ± 8	0 ± 11
5. Discrete charge	0 ± 10	0 ± 2	0 ± 2	0 ± 2	···	0 ± 10	0 ± 2	0 ± 2
Total	-110 ± 85	-27 ± 25	-40 ± 32	-34 ± 30	-9 ± 13	$+75\pm65$	$+7\pm25$	$+27\pm25$

probably a generous estimate for the uncertainty in the effect on the $1S$ state. The $2S$ state is also lowered by the nuclear polarization effect, by a lesser amount. Roughly, the ratio of $2S$ to $1S$ energy shift is equal to the ratio of $2S$ and $1S$ meson densities within the nucleus, or about 1/6. Using the same crude method to estimate the polarization effect on the $2P$ states, we find $\Delta E(2P_{1/2})/\Delta E(1S)\cong 1/7$, $\Delta E(2P_{3/2})/\Delta E(1S)\cong 1/12$, and $\Delta E(3D)$ negligible (less than 1 kev).

(f) *Mass of muon.* In the vicinity of the "true" radius, the calculated energies may be written

$$(E/mc^2)\sim(r_0/\lambda\!\!\!^{-}_{\mu})^a,$$

where m and $\lambda\!\!\!^{-}_{\mu}$ are the mass and reduced Compton wavelength of the muon. For fixed radial constant, therefore,

$$E\sim m^{a+1}.$$

Values of the exponent a for the binding energies and transition energies are given in Table I. The $2P\rightarrow 1S$ transitions are insensitive to meson mass. At somewhat larger radii, $a+1$ is even closer to zero.[4,5] We have chosen $m=207.0m_e$[15] and placed arbitrary limits of error of $\pm 1m_e$ on this value in order to determine the uncertainties given in Table III.

(g) *Nuclear quadrupole moment.* For a zero-spin nucleus, a nuclear deformation changes slightly the effective shape of the nuclear charge distribution,[16] and in particular extends the mean radius fractionally by about $(3/5)\alpha^2$, where α is a deformation parameter defined by

$$R=R_0[1+\alpha P_2(\cos\theta)].$$

For a nucleus with nonzero spin, the center of gravity of the hyperfine structure pattern reacts in the same way to the effective rounding of the edge of the charge distribution and the slight extension of the nucleus. (Wheeler[3] has considered quadrupole hyperfine patterns.) Some nuclei may have values of α as great as 0.25 but a probable upper limit for Pb^{207} is 0.05. Since for Pb the $1S$ energy varies roughly as $R^{-0.5}$, an upper limit for the quadrupole energy shift for the $1S$ state of Pb^{207} is about 5 kev. Pb^{208} is expected to have no quadrupole effect (although the zero point surface vibration will act in the same way to extend[17] slightly the charge distribution).

(h) *Granularity of nuclear charge.* Cooper and Henley[5] estimate the effect of the discrete charge distribution on the $1S$ state of Pb to be less than 10 kev. We have not attempted to improve on this estimate. The effect on the $2S$ and $2P$ levels will be smaller than the $1S$ effect by a factor of 5 to 10.

(i) *Electron shielding.* The number of K electrons within a radius of three nuclear radii is about 0.9×10^{-4}. If the total electron charge in the same volume is generously taken to be ten times this number, the total fractional effect of electrons on the potential seen by the mesons is about 10^{-5}, and may be ignored.

The relevant perturbations are summarized in Table III. We conclude that the $2P\rightarrow 1S$ transition energies can be calculated to within about 65 kev, and the $3D\rightarrow 2P$ and $2S\rightarrow 2P$ transitions to within about 25 kev. Since the $2P_{1/2}$ and $2P_{3/2}$ states are similarly perturbed by most effects, the uncertainty in the determination of the $2P$ doublet splitting is only about 5 kev. As is discussed in Part IV, these uncertainties are small enough that the possibility exists to determine in a certain sense the shape as well as the size of the nuclear charge distribution from the low mu-mesonic transitions alone.

There is strong reason to believe, therefore, that the mu meson is a probe particle sensitive to the extent of the nuclear charge distribution but relatively free of uncertainty in theoretical interpretation of transition energies.[3] As a nucleus to probe, Pb appears ideal, and we have restricted our calculations to this element. It has the greatest spacing of low-lying levels among the heavy nuclei, which serves to minimize the nuclear polarization effect. Its ground-state deformation is small. It has been already investigated with mu mesons[4] and with high energy electrons[7] and its isotope shift has been measured[18] and analyzed.[19] It is an experimentally convenient substance with which to work. It has only the disadvantage of possessing several isotopes. For future precise determinations of the mu-mesonic $2P$ fine structure splitting, for example, Au or separated Pb^{208} would be preferable.

[15] Smith, Birnbaum, and Barkas, Phys. Rev. **91**, 765 (1953).
[16] Wilets, Hill, and Ford, Phys. Rev. **91**, 1488 (1953).
[17] D. L. Hill and J. A. Wheeler, Phys. Rev. **89**, 1102 (1953).
[18] Brix, von Buttlar, Houtermans, and Kopfermann, Z. Physik **133**, 192 (1952); other references there.
[19] P. Brix and H. Kopfermann, Festschr. Akad. Wiss., Göttingen, Math.-Physik Kl. **17** (1951); Phys. Rev. **85**, 1050 (1952).

III. EXACT CALCULATIONS

Dimensionless Formulation

We consider families of charge distributions of the form

$$\rho(r)=\rho_0 f_\lambda(x), \quad x\equiv r/r_0. \tag{5}$$

Here ρ_0 is the central charge density, $f_\lambda(0)=1$; λ represents any number of parameters used to define the shape of the distribution, and r_0, the range parameter, defines the radial extent of the distribution. We define the functionals of f:

$$I_f(x)=\int_0^x f(x)x^2dx; \tag{6}$$

$$J_f(x)=[I_f(\infty)]^{-1}\int_0^x I_f(x)x^{-2}dx. \tag{7}$$

Then the normalizing condition is

$$4\pi r_0^3\rho_0 I_f(\infty)=Ze, \tag{8}$$

and the electrostatic potential is

$$V=-(Ze/r_0)J_f(x). \tag{9}$$

We further define the dimensionless energy $\epsilon=E/mc^2$, where $m=$mu-meson mass$=207m_e$, and the dimensionless range parameter, $\gamma=r_0/\lambda\!\!\!^{-}_\mu$, where $\lambda\!\!\!^{-}_\mu=\hbar/mc$ =reduced Compton wavelength of the mu meson. Then the radial equations for the Dirac particle in a central field[20] become

$$\begin{aligned} dG/dx&=-(k/x)G+[\gamma(\epsilon+1)+\alpha ZJ_f(x)]F,\\ dF/dx&=(k/x)F-[\gamma(\epsilon-1)+\alpha ZJ_f(x)]G, \end{aligned} \tag{10}$$

where F/x and G/x are the two components of the wave function and k is the angular quantum number. For the six levels considered, $k=-1(1S$ and $2S)$, $+1(2P_{1/2})$, $-2(2P_{3/2})$, $+2(3D_{3/2})$, and $-3(3D_{5/2})$.

Families of Charge Distributions

In order to cover the landscape of possible charge distributions, we have considered several members of each of four families of distributions.

Family I

$$f_n(x)=(1/n!)\int_x^\infty x^n e^{-x}dx=\sum_{k=0}^{n}\frac{x^k}{k!}e^{-x}, \quad n=0,1,2\cdots. \tag{11}$$

For $n=0$, this is an exponential, for $n=1$, a modified exponential (name used by Schiff[8]). As $n\to\infty$, f approaches a square distribution, but the high-n members of the family are not feasible for calculation.

For this and the succeeding families, the charge normalization integral $I_f(\infty)$ [Eq. (6)] and the dimensionless potential $J_f(x)$ [Eq. (7)] are given in Appendix I.

[20] L. I. Schiff, *Quantum Mechanics* (McGraw-Hill Book Company, New York, 1949), p. 319.

Family II

$$\text{(a)}\quad f_n(x)=\frac{1}{1-\frac{1}{2}e^{-n}}\cdot\begin{cases}1-\frac{1}{2}e^{-n}e^{x}, & x\leqslant n\\ \frac{1}{2}e^{n}e^{-x}, & x\geqslant n\end{cases}, \quad 0\leqslant n\leqslant 1. \tag{12}$$

As n varies from 0 to 1, f varies from an exponential toward a shape roughly Gaussian in appearance.

$$\text{(b)}\quad f_n(x)=\frac{1}{1-\frac{1}{2}e^{-n}}\cdot\begin{cases}1-\frac{1}{2}e^{-n(1-x)}, & x\leqslant 1\\ \frac{1}{2}e^{-n(x-1)}, & x\geqslant 1\end{cases}, \quad 1\leqslant n<\infty. \tag{13}$$

As n varies from 1 to infinity, f varies from a shape roughly Gaussian in appearance to a square shape (uniform distribution). Families IIa and IIb form a single connected family (being identical at $n=1$), but are distinguished in order that the range parameter r_0 may have a close relation to the size of the nucleus. For family IIa, the relevant distance is the decay length for $x>n$. For family IIb, the relevant distance is the interval out to the point where the distribution begins to fall exponentially.

Family III

$$f_{ns}(x)=\frac{\sinh sx/sx}{1-\frac{1}{2}e^{-n}}\cdot\begin{cases}1-\frac{1}{2}e^{-n(1-x)}, & x\leqslant 1\\ \frac{1}{2}e^{-n(x-1)}, & x\geqslant 1\end{cases}, \quad n\geqslant 1,\ n>s. \tag{14}$$

This family is a generalization of family IIb and includes shapes peaked at the edge of the nucleus instead of at the center. It leads to complicated formulas, but is worth examining to discover if previous ideas about a slight depression of central charge density[21–23,16] relative to the outer part of the nucleus must be discarded.

Family IV

This family is made of various separate simple distributions, some of which are special cases of the previous three families.

A. Exponential: $f=e^{-x}$, (15)

B. Modified exponential: $f=(1+x)e^{-x}$, (16)

C. Gaussian: $f=\exp(-x^2)$, (17)

D. Modified Gaussian: $f=(1+x^2)\exp(-x^2)$, (18)

E. Square: $f=1, x<1; f=0, x>1$. (19)

Another distribution of interest for Pb is that derived theoretically by Gombas[24] from a statistical treatment:

$$f_G=(1+0.15x^2)^3\exp(-x^2). \tag{20}$$

[21] E. Wigner, Bicentennial Symposium, University of Pennsylvania, 1940 (unpublished).
[22] E. Feenberg, Phys. Rev. **59**, 593 (1941).
[23] W. J. Swiatecki, Proc. Phys. Soc. (London) **A63**, 1208 (1950).
[24] P. Gombas, Acta Phys. Acad. Sci. Hung. **1**, 329 (1952) and **2**, 223 (1952).

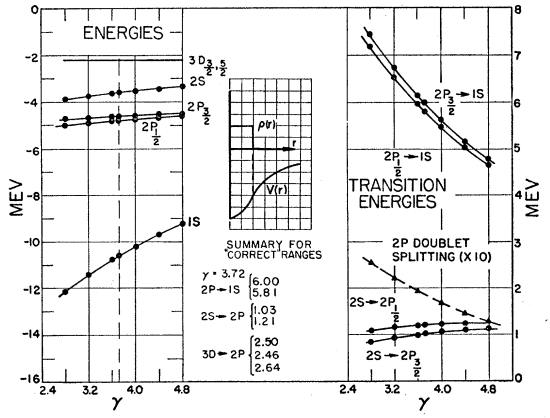

FIG. 1. Binding energies, transition energies, and $2P$ doublet splitting for the uniform charge distribution. Energies are given in Mev, assuming a meson mass of $207.0m_e$, and are plotted *vs* γ, the nuclear radius in units of the meson reduced Compton wavelength. The $3D$ levels were calculated by perturbation theory. The vertical dashed lines indicate the radius for which $2P_{3/2}\rightarrow 1S$ energy equals 6.00 Mev.

This distribution is approximately represented by intermediate members of families I and II.

Solution for Energy Levels

With the aid of one of the Los Alamos I.B.M. Type-701 electronic computers, and of its staff,[25] we have solved the radial equations (6) for various charge distributions $f(x)$ and various range parameters γ. For each choice of shape $[f(x)]$ and size (γ), the equations have been solved by successive trials with ϵ, the energy, as the eigenvalue. Some remarks on the numerical procedure are contained in an appendix. The energy values obtained are accurate to about 10^{-4} Mev.

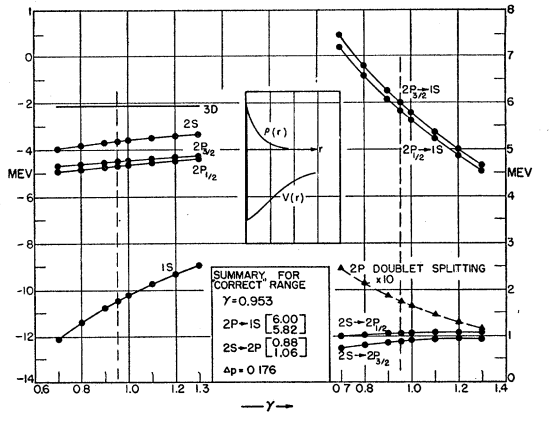

FIG. 2. Binding energies, transition energies, and $2P$ doublet splitting for the exponential charge distribution, plotted in the same way as Fig. 1. Graphs for shapes of charge distribution intermediate between uniform and exponential are qualitatively the same as Figs. 1 and 2.

[25] We express our appreciation, in particular, to Mr. Richard G. Clow and to Mr. John T. Mann for their valuable assistance on several occasions in operation of the computer.

The wave functions and energy values were found for the four lowest states. For each shape, the energy eigenvalues have been found for several ranges such that the experimental $2P_{3/2}\rightarrow 1S$ transition energy of 6 Mev is bracketed, with calculations extending to transition energies 20 percent greater and 20 percent smaller than 6 Mev.

The $3D$ levels have been calculated by perturbation theory, since the finite nucleus effect on these levels is small. The first order energy shifts away from the Dirac point nucleus values were calculated for the exponential charge distribution at the radius giving a $2P_{3/2}\rightarrow 1S$ transition energy of 6.00 Mev. The rate of variation of the energy shift with radius was found at the same point. At this radius, the $3D_{3/2}$ state is shifted by 14.9 kev and the shift varies as $r_0^{3.89}$. The $3D_{5/2}$ state is shifted by 5.7 kev and the shift varies as $r_0^{4.13}$. The energy shifts for the uniform distribution were found by assuming that the shift varies roughly as $\langle r^4\rangle_{\text{Av}}$ for different shapes of charge distribution. This crude approximation is adequate because the shifts for the uniform distribution are so small—3 ± 1 kev for the $3D_{3/2}$ state and 1 ± 0.5 kev for the $3D_{5/2}$ state. Although the $3D$ levels are insensitive to the extent of the nuclear charge, the $3D\rightarrow 2P$ transition does probe the nucleus in an important way. The $3D\rightarrow 2P$ transition should be strong. There is doubt whether the $2S\rightarrow 2P$ transition will be observable, due to the small occupation of the $2S$ state.

IV. RESULTS

In Figs. 1 and 2, sample energy level results for Pb are presented graphically. For each assumed shape of charge distribution, the lowest six energy levels are plotted as a function of the range parameter γ. The energies are given in Mev, assuming a mu-meson mass of 207.0 electron masses.[15] Since only E/mc^2 is determined by the solutions, the energies may be readily (but not linearly) scaled for a possible correction to the mu-meson mass. The dimensionless range parameter γ is equal to the range parameter r_0 divided by λ_μ, the reduced Compton wavelength of the mu meson, 1.8665 $\times 10^{-13}$ cm for the assumed mass of $207.0m_e$, and including a reduced mass correction.

The binding energies given in Figs. 1 and 2 and all other exactly calculated energies are presented tabularly in Table IV. The lowest four energies and transition energies are summarized in Table V for fixed $2P_{3/2}\rightarrow 1S$ transition energy. In Table VI are given the $3D$ energies and transitions, subject to the same condition, for the uniform and exponential distributions. The $3D\rightarrow 2P$ transition energies for intermediate shapes may readily be interpolated, since the major variation comes from the P states.

It is of fundamental interest to know whether the $2P$ doublet splitting and the $3D\rightarrow 2P$ and $2S\rightarrow 2P$ energies, taken together with the $2P\rightarrow 1S$ energies, can provide information on the shape of the charge distribution.

TABLE IV. All exactly calculated binding energies. The lines prefaced by arrows have in common a $2P_{3/2}\rightarrow 1S$ transition energy of 6.00 Mev. Families I through IV are defined by Eqs. (5) through (19).

Shape parameter	Range parameter γ	Binding energies in Mev $1S$	$2S$	$2P_{1/2}$	$2P_{1/2}$
		Family I			
$n=0$	0.7000	12.114	3.914	4.913	4.668
	0.8000	11.416	3.790	4.823	4.608
	0.9000	10.802	3.679	4.732	4.543
→	0.9529	10.504	3.624	4.684	4.508
	1.0000	10.257	3.577	4.641	4.475
	1.1000	9.769	3.485	4.552	4.405
	1.2000	9.330	3.399	4.465	4.334
	1.3000	8.932	3.320	4.379	4.263
$n=1$	0.5600	12.117	3.908	4.927	4.680
	0.6400	11.413	3.783	4.838	4.623
	0.7200	10.792	3.669	4.749	4.560
→	0.7577	10.525	3.620	4.706	4.529
	0.8000	10.242	3.567	4.659	4.493
	0.8800	9.749	3.473	4.571	4.424
	0.9600	9.305	3.386	4.484	4.354
	1.0400	8.904	3.306	4.399	4.283
$n=2$	0.4667	12.122	3.905	4.936	4.689
	0.5333	11.412	3.778	4.849	4.633
	0.6000	10.788	3.663	4.761	4.571
→	0.6289	10.539	3.616	4.722	4.543
	0.6667	10.233	3.559	4.672	4.506
	0.7333	9.737	3.465	4.585	4.438
	0.8000	9.290	3.377	4.498	4.368
	0.8667	8.886	3.297	4.413	4.298
$n=3$	0.4000	12.126	3.902	4.944	4.695
	0.4571	11.413	3.774	4.857	4.640
	0.5143	10.785	3.659	4.770	4.580
→	0.5376	10.550	3.615	4.734	4.554
	0.5714	10.228	3.554	4.682	4.515
	0.6286	9.729	3.458	4.595	4.448
	0.6857	9.280	3.371	4.509	4.379
	0.7429	8.874	3.289	4.424	4.309
$n=4$	0.3500	12.130	3.900	4.949	4.699
	0.4000	11.414	3.771	4.863	4.646
	0.4500	10.784	3.655	4.777	4.586
→	0.4695	10.558	3.613	4.743	4.562
	0.5000	10.224	3.550	4.690	4.523
	0.5500	9.724	3.454	4.603	4.456
	0.6000	9.273	3.365	4.517	4.388
	0.6500	8.865	3.284	4.433	4.318
$n=6$	0.2800	12.136	3.898	4.957	4.706
	0.3200	11.417	3.767	4.873	4.654
	0.3600	10.783	3.650	4.787	4.596
→	0.3746	10.570	3.610	4.755	4.574
	0.4000	10.220	3.544	4.701	4.534
	0.4400	9.717	3.447	4.615	4.468
	0.4800	9.264	3.358	4.529	4.400
	0.5200	8.854	3.275	4.445	4.331
$n=\infty$	2.8000[a]	12.177	3.888	4.991	4.735
	3.2000	11.442	3.752	4.913	4.690
	3.6000	10.793	3.630	4.833	4.639
→	3.7159	10.619	3.596	4.809	4.623
	4.0000	10.217	3.518	4.752	4.583
	4.4000	9.701	3.417	4.670	4.522
	4.8000	9.237	3.323	4.588	4.459
		Family II			
$n=0.5$	0.7200	11.965	3.888	4.895	4.657
	0.9000	10.800	3.678	4.731	4.543
→	0.9536	10.500	3.623	4.683	4.507
	1.0800	9.861	3.502	4.570	4.419
	1.2600	9.085	3.351	4.413	4.291
	1.4400	8.433	3.218	4.263	4.163
	1.6200	7.876	3.100	4.120	4.038
	1.8000	7.394	2.993	3.985	3.916

Shape parameter	Range parameter γ	Binding energies in Mev $1S$	$2S$	$2P_{1/2}$	$2P_{3/2}$
		Family II			
$n=1$	0.6600	12.397	3.963	4.947	4.690
	0.7700	11.592	3.821	4.848	4.626
	0.8800	10.894	3.695	4.747	4.555
→	0.9480	10.507	3.623	4.686	4.510
	0.9900	10.283	3.582	4.648	4.481
	1.1000	9.744	3.479	4.549	4.403
	1.2100	9.263	3.385	4.453	4.325
	1.3200	8.832	3.299	4.359	4.246
$n=2$	1.2000	12.647	4.002	4.983	4.713
	1.4000	11.837	3.859	4.890	4.656
	1.6000	11.133	3.732	4.796	4.593
→	1.7976	10.522	3.620	4.703	4.525
	1.8000	10.515	3.618	4.702	4.525
	2.0000	9.9676	3.515	4.608	4.453
	2.2000	9.4791	3.420	4.516	4.380
	2.4000	9.0401	3.333	4.426	4.305
$n=4$	1.9600	12.499	3.963	4.993	4.726
	2.2400	11.782	3.834	4.915	4.680
→	2.8071	10.568	3.609	4.753	4.572
	3.0801	10.074	3.515	4.675	4.514
	3.3601	9.616	3.426	4.595	4.452
	3.6401	9.200	3.343	4.516	4.389
	3.9201	8.821	3.266	4.438	4.324
$n=10$	2.4500	12.584	3.966	5.024	4.750
	2.8000	11.855	3.833	4.952	4.711
	3.1500	11.209	3.713	4.877	4.665
	3.5000	10.632	3.604	4.801	4.615
→	3.5147	10.609	3.599	4.798	4.613
	3.8500	10.115	3.504	4.725	4.561
	4.2000	9.647	3.412	4.648	4.503
	4.5500	9.223	3.327	4.508	4.377
	4.9000	8.836	3.248	4.495	4.381
$n=\infty$	Same as Family I.				

n	s	γ	$1S$	$2S$	$2P_{1/2}$	$2P_{3/2}$
		Family III				
4	2	1.4400	12.568	3.984	4.980	4.713
		1.6800	11.752	3.840	4.887	4.656
		1.9200	11.044	3.711	4.793	4.5920
	→	2.1144	10.534	3.616	4.716	4.537
		2.1600	10.422	3.594	4.698	4.524
		2.4000	9.872	3.489	4.604	4.452
		2.6400	9.381	3.392	4.512	4.379
		2.8800	8.940	3.304	4.421	4.304
5.3	2	1.9600	12.260	3.918	4.971	4.714
		2.2400	11.539	3.788	4.889	4.665
		2.5200	10.903	3.670	4.806	4.610
	→	2.6791	10.574	3.608	4.759	4.577
		2.8000	10.338	3.563	4.723	4.551
		3.0800	9.831	3.465	4.640	4.488
		3.3600	9.375	3.374	4.557	4.423
		3.6400	8.962	3.291	4.475	4.357
8	1.5	2.4500	12.170	3.892	4.981	4.726
		2.8000	11.439	3.758	4.901	4.679
		3.1500	10.795	3.637	4.819	4.626
	→	3.2628	10.603	3.600	4.792	4.607
		3.5000	10.223	3.527	4.736	4.567
		3.8500	9.711	3.427	4.653	4.506
		4.2000	9.250	3.334	4.570	4.441
		4.5500	8.833	3.249	4.488	4.374

[a] For uniform distribution ($n=\infty$) $\gamma=R/\lambda c$.

TABLE IV.—*Continued.*

Shape parameter		Range parameter γ	Binding energies in Mev $1S$	$2S$	$2P_{1/2}$	$2P_{3/2}$
			Family III			
8	2	2.4000	12.112	3.882	4.975	4.723
		2.7000	11.467	3.763	4.904	4.681
		3.0000	10.891	3.655	4.832	4.634
	→	3.1614	10.605	3.601	4.793	4.608
		3.3000	10.372	3.556	4.759	4.584
		3.6000	9.903	3.464	4.685	4.530
		3.9000	9.476	3.380	4.612	4.474
		4.2000	9.086	3.301	4.539	4.416
8	3	2.2400	12.065	3.874	4.969	4.719
		2.5600	11.335	3.739	4.887	4.670
		2.8800	10.692	3.617	4.803	4.615
	→	2.9276	10.602	3.600	4.791	4.606
		3.2000	10.120	3.507	4.719	4.555
		3.5200	9.610	3.406	4.634	4.491
		3.8400	9.150	3.314	4.550	4.425
12	1.5	2.4500	12.512	3.951	5.020	4.749
		2.8000	11.780	3.817	4.947	4.709
		3.1500	11.133	3.696	4.872	4.663
	→	3.4616	10.615	3.598	4.804	4.618
		3.5000	10.555	3.586	4.796	4.612
		3.8500	10.037	3.485	4.718	4.557
		4.2000	9.569	3.393	4.641	4.499
		4.5500	9.145	3.307	4.564	4.438
12	1.8	2.4500	12.448	3.939	5.015	4.747
		2.8000	11.715	3.805	4.941	4.706
		3.1500	11.067	3.684	4.865	4.659
	→	3.4200	10.616	3.598	4.805	4.619
		3.5000	10.490	3.573	4.787	4.607
		3.8500	9.972	3.472	4.709	4.551
		4.2000	9.505	3.379	4.631	4.491
		4.5500	9.081	3.293	4.553	4.430
12	2	2.4500	12.402	3.930	5.011	4.745
		2.8000	11.669	3.796	4.936	4.703
		3.1500	11.021	3.674	4.859	4.655
	→	3.3904	10.617	3.597	4.806	4.620
		3.5000	10.443	3.564	4.781	4.603
		3.8500	9.926	3.463	4.702	4.546
		4.2000	9.459	3.370	4.624	4.486
		4.5500	9.036	3.284	4.545	4.424
			Family IV			
		γ	$1S$	$2S$	$2P_{1/2}$	$2P_{3/2}$
Gaussian		1.8200	12.211	3.934	4.967	4.714
		2.0800	11.496	3.807	4.884	4.663
		2.3400	10.865	3.692	4.800	4.607
	→	2.4714	10.573	3.638	4.757	4.576
		2.6000	10.305	3.588	4.716	4.546
		2.8600	9.803	3.493	4.631	4.482
		3.1200	9.351	3.406	4.547	4.415
		3.3800	8.941	3.326	4.465	4.348
Modified Gaussian		1.4700	12.396	3.970	4.995	4.733
		1.6800	11.677	3.841	4.917	4.687
		1.8900	11.041	3.726	4.837	4.635
	→	2.0560	10.588	3.642	4.774	4.591
		2.1000	10.475	3.621	4.757	4.579
		2.3100	9.967	3.525	4.676	4.519
		2.5200	9.509	3.437	4.596	4.457
		2.7300	9.094	3.356	4.515	4.393

TABLE V. Summary of exactly calculated energies at radii chosen to yield $2P_{3/2}\rightarrow 1S$ energy $\cong$6.00 Mev. The indices n and s designate the shape of the charge distribution. The range parameter measures the size. All energies in Mev.

n	s	γ	$1S$	$2S$	$2P_{1/2}$	$2P_{3/2}$	$2P_{3/2}\rightarrow 1S$	$2P_{1/2}\rightarrow 1S$	$2S\rightarrow 2P_{3/2}$	$2S\rightarrow 2P_{1/2}$	ΔP
					Family I						
0		0.9529	10.504	3.623	4.684	4.508	5.997	5.821	0.884	1.060	0.176
1		0.7577	10.525	3.620	4.706	4.529	5.997	5.819	0.909	1.086	0.178
2		0.6289	10.540	3.617	4.722	4.543	5.997	5.818	0.926	1.105	0.179
3		0.5376	10.551	3.615	4.734	4.554	5.997	5.817	0.939	1.119	0.180
4		0.4695	10.559	3.613	4.743	4.562	5.997	5.816	0.949	1.130	0.181
6		0.3746	10.570	3.610	4.755	4.574	5.997	5.815	0.963	1.145	0.182
∞		3.7159	10.620	3.596	4.809	4.623	5.997	5.810	1.027	1.213	0.186
					Family II						
0.5		0.9536	10.500	3.623	4.683	4.507	5.993	5.817	0.884	1.060	0.176
1.0		0.9480	10.507	3.623	4.685	4.509	5.998	5.822	0.886	1.062	0.176
2.0		1.7976	10.522	3.619	4.703	4.525	5.997	5.819	0.906	1.083	0.177
4.0		2.8071	10.568	3.609	4.753	4.572	5.997	5.815	0.962	1.144	0.182
10.0		3.5147	10.609	3.599	4.798	4.613	5.997	5.811	1.013	1.199	0.186
					Family III						
n	s										
4	2	2.1144	10.534	3.615	4.716	4.537	5.997	5.818	0.922	1.101	0.179
5.3	2	2.6791	10.574	3.608	4.759	4.577	5.998	5.815	0.969	1.151	0.182
8	2	3.1614	10.605	3.601	4.792	4.608	5.997	5.813	1.007	1.192	0.185
8	1.5	3.2628	10.603	3.600	4.792	4.607	5.996	5.811	1.007	1.192	0.185
8	3	2.9276	10.602	3.600	4.791	4.606	5.996	5.811	1.006	1.191	0.185
12	1.5	3.4616	10.615	3.598	4.804	4.618	5.997	5.811	1.020	1.206	0.186
12	1.8	3.4200	10.616	3.598	4.805	4.619	5.997	5.811	1.021	1.207	0.186
12	2	3.3904	10.617	3.597	4.806	4.620	5.997	5.811	1.022	1.208	0.186
					Family IV						
Gaussian		2.4714	10.573	3.638	4.758	4.576	5.997	5.816	0.938	1.119	0.181
Modified Gaussian		2.0560	10.588	3.642	4.774	4.591	5.997	5.815	0.949	1.132	0.182

TABLE VI. $3D$ binding energies and transition energies for uniform and exponential distributions, with radii chosen as in Table V. Energies in Mev.

n	$3D_{5/2}$	$3D_{3/2}$	$3D_{5/2}\rightarrow 2P_{3/2}$	$3D_{3/2}\rightarrow 2P_{3/2}$	$3D_{3/2}\rightarrow 2P_{1/2}$	Δ_D
0	2.119	2.155	2.389	2.353	2.529	0.036
∞	2.124	2.167	2.499	2.456	2.642	0.034

Figures 3 and 4 present the $3D\rightarrow 2P$ and $2S\rightarrow 2P$ transition energies and the $3D$ and $2P$ doublet splitting as a function of a suitable shape parameter for families I and II, subject to the restriction that the $2P_{3/2}\rightarrow 1S$ transition energy is 6.0 Mev. Future experiments may of course alter the value of the $2P_{3/2}\rightarrow 1S$ energy, in which case interpolation in Table III would be required, but for illustrative purposes, it is adequate to take 6.00 Mev for this transition energy and to investigate to what extent the other transitions among the low states may reveal more about the nuclear charge distribution.

Table III indicates that a calculated $2P_{3/2}\rightarrow 1S$ transition energy of 5.997 Mev corresponds to an observed transition energy of 6.072 ± 0.065 Mev. Conversely, a measured energy of 6.07 Mev corresponds to a calculated energy of 6.00 ± 0.07 Mev, which implies an uncertainty in the determination of the radial constant for any shape of charge distribution of about 1.3 percent. (It is assumed that the uncertainty in the experimental measurement is small compared to the 65 kev theoretical uncertainty.) Table I shows the relative

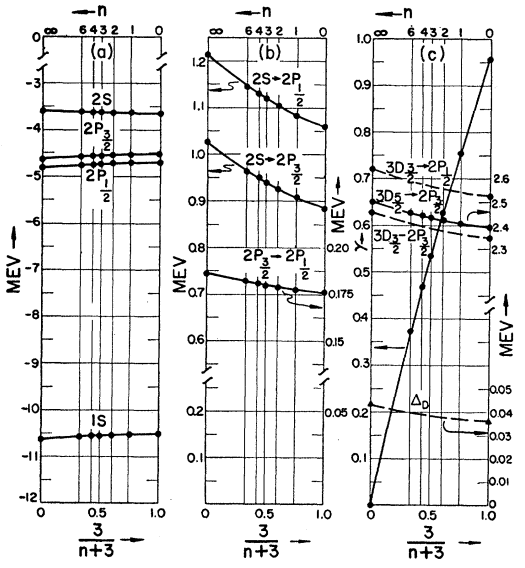

FIG. 3. Energies *vs* shape of charge distribution for family I, limited by the condition $2P_{3/2}\rightarrow 1S$ energy = 6.00 Mev. (a) Binding energies of four lowest states. (b) $2S\rightarrow 2P$ transition energies and $2P$ doublet splitting. (c) $3D\rightarrow 2P$ transition energies, $3D$ doublet splitting, and range parameter γ. The quantities are plotted *vs* an arbitrarily chosen shape parameter, $3/(n+3)$, which runs from 0 (uniform distribution) to 1 (exponential distribution).

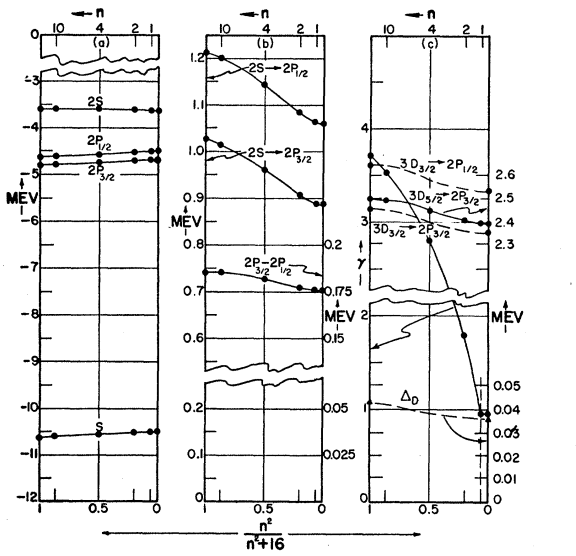

FIG. 4. Energies and radii *vs* shape of charge distribution for family II limited by the condition $2P_{3/2}\rightarrow 1S$ energy = 6.00 Mev. (a) Binding energies of four lowest states. (b) $2S\rightarrow 2P$ transition energies and $2P$ doublet splitting. (c) $3D\rightarrow 2P$ transition energies, $3D$ doublet splitting, and range parameter γ. The quantities are plotted *vs* an arbitrarily chosen shape parameter, $n^2/(n^2+16)$, which runs from 1 (uniform distribution) to 0 (exponential distribution).

sensitivity of the various measurable energies to a change of nuclear radius. For the present example, we assume a distribution intermediate between uniform and exponential. Then the 1.3 percent uncertainty in radius implies uncertainties of about 0.22 percent in the $3D\rightarrow 2P_{3/2}$ transition, 0.60 percent in the $2S\rightarrow 2P_{3/2}$ transition, and 0.26 percent in the $2S\rightarrow 2P_{1/2}$ transition. To these uncertainties must be added the (larger) theoretical uncertainty of about 25 kev from Table III. Finally then, the $3D\rightarrow 2P$ transition energies are pre-

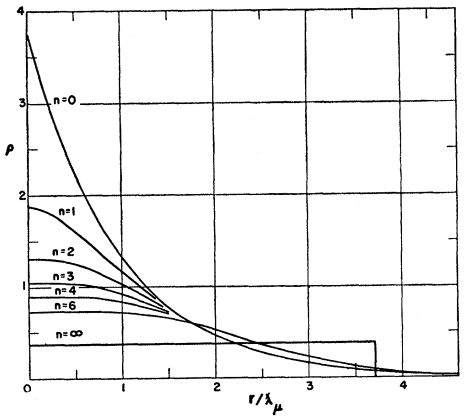

FIG. 5. "Equivalent" charge distributions for family I, for each of which the $2P_{3/2}\rightarrow 1S$ transition energy = 6.00 Mev. The horizontal scale is in units of the meson reduced Compton wavelength, $\lambda\!\!\!^{-}_{\mu}$. The vertical scale is in number of protons per $\lambda\!\!\!^{-}_{\mu}{}^3$. The range parameters for these distributions are given in Table IV and plotted in Fig. 3.

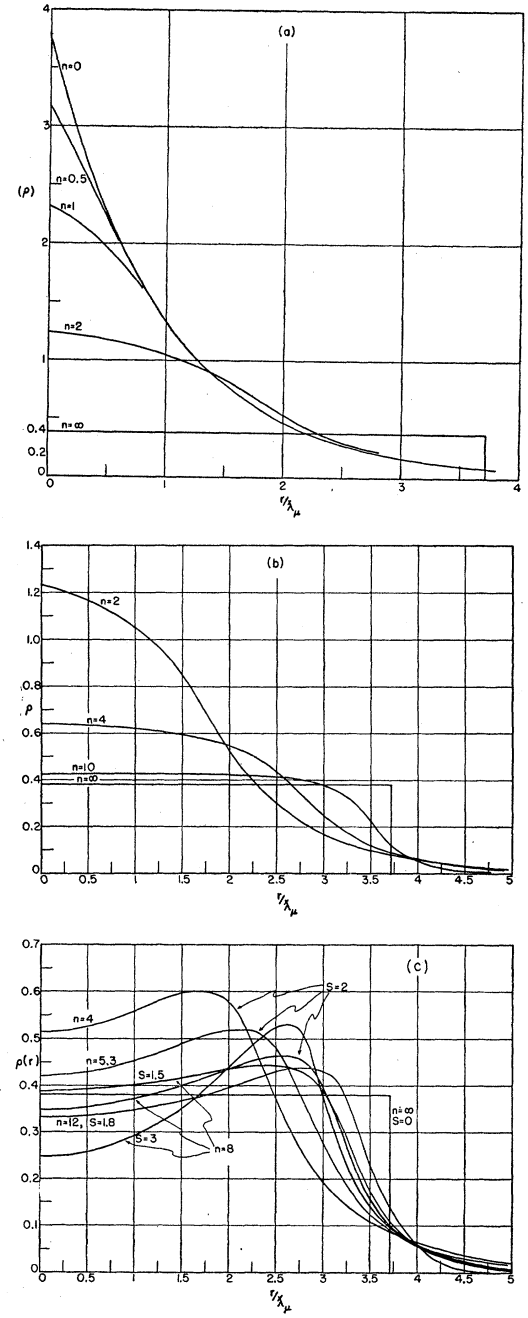

FIG. 6. "Equivalent" charge distributions for families II and III, for each of which the $2P_{3/2}\rightarrow 1S$ transition energy = 6.00 Mev. The horizontal scale is in units of the meson reduced Compton wavelength, $\lambda\!\!\!^{-}_{\mu}$. The vertical scale in number of protons per $\lambda\!\!\!^{-}_{\mu}{}^{3}$. The range parameters for these distributions are given in Table IV and plotted in Fig. 4.

dictable to within about 1.2 percent, and the $2S\rightarrow 2P$ energies to about 3 percent, for any assumed shape of charge distribution from an experimental $2P_{3/2}\rightarrow 1S$ energy measured to within a few tens of kev. The sensitivity of these transition energies to change of shape is considerably greater, however (see Figs. 3 and 4 and Tables V and VI). The change from uniform to exponential changes the $3D\rightarrow 2P$ energies by about 4.5 percent and the $2S\rightarrow 2P$ energies by about 15 percent. It therefore appears that a knowledge of these mesonic transition energies could throw considerable light on the shape of the nuclear charge distribution.

The $2P$ doublet splitting, on the other hand, is sensitive both to the radius and to the shape of the charge distribution. A 1.3 percent uncertainty in the radius introduces about a 1.6 percent uncertainty in the $2P$ doublet splitting, while the change of shape from uniform to exponential alters the $2P$ doublet splitting by about 10 kev or 5.5 percent. The determination of the $2P$ doublet splitting,[26] e.g., via the $3D\rightarrow 2P$ transitions, would be most useful in providing an independent sensitive measurement of the nuclear radius and checking for the possible existence of an anomalous muon magnetic moment. The $3D$ doublet splitting, although small ($\sim$40 kev), is sensitive to the shape of the charge distribution (Fig. 3). Its determination would provide another useful datum on which to base a firm picture of the nuclear charge distribution.

Figures 5 and 6 show the set of equivalent charge distributions for which the $2P_{3/2}\rightarrow 1S$ transition energy is 6.00 Mev. Figure 7 shows the corresponding equivalent potentials for the extreme case of uniform and exponential distributions. Sample normalized wave functions are shown in Fig. 8 for the uniform distribution. The wave functions vary little from one distribution to another, as is illustrated by the differences between uniform and exponential wave functions shown in part (c) of Fig. 8. Additional detailed numerical results are available from the authors.

The sensitivity of the transition energies to the distribution of nuclear charge may be seen in a more

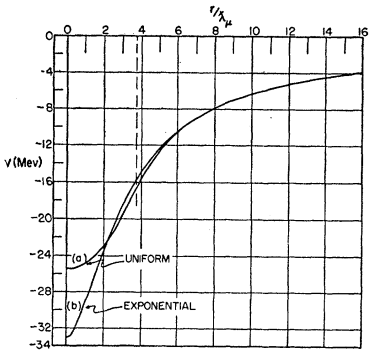

FIG. 7. "Equivalent" potentials for the uniform and exponential charge distributions, for each of which the $2P_{3/2}\rightarrow 1S$ transition energy = 6.00 Mev. (a) Potential of uniform distribution, with nuclear radius indicated by dashed line. (b) Potential of exponential distribution. Vertical scale in Mev, assuming a meson mass of $207.0m_e$. Horizontal scale in units of meson reduced Compton wavelength, $\lambda\!\!\!^{-}_{\mu}$. Corresponding charge distributions given in Figs. 5 and 6.

[26] Preliminary measurements [J. Rainwater, Phys. Rev. **94**, 773(T) (1954)] indicate a $2P$ doublet splitting of 0.18 Mev.

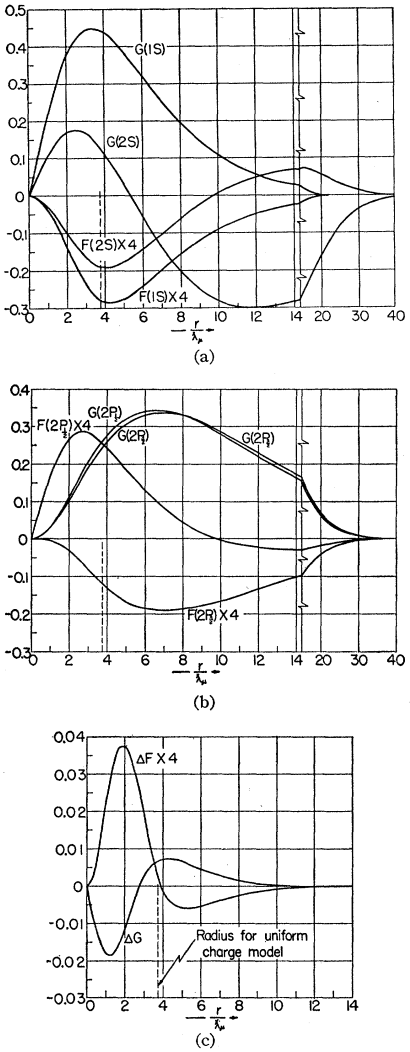

FIG. 8. Normalized wave functions. The horizontal scale is in units of the meson reduced Compton wavelength, $\lambda\!\!\!^{-}_{\mu}$. The normalization is: $(1/\lambda\!\!\!^{-}_{\mu})\int_0^\infty(F^2+G^2)dr=1$. (a) Wave functions for $1S$ and $2S$ states, uniform charge distribution, radius $R=3.716\lambda\!\!\!^{-}_{\mu}$. (b) Wave functions for $2P$ states, same charge distribution. (c) Comparison of $1S$ state wave functions for the "equivalent" uniform and exponential potentials illustrated in Fig. 7. The differences $\Delta F=F_{\text{unif}}-F_{\text{exp}}$ and $\Delta G=G_{\text{unif}}-G_{\text{exp}}$ are plotted.

pictorial way by using perturbation theory to examine the effect of changes in the charge distribution away from the uniform distribution with "correct" radius. If the altered charge distribution is $\rho_{\text{unif}}+\delta\rho(r)$, the energy shift of the mth level is

$$\Delta E_m=+4\pi\int_0^\infty v_m(r)\delta\rho(r)r^2dr, \tag{21}$$

where $v_m(r)$, the effective potential due to mu meson in the mth state (adjusted to zero at the origin), is given by

$$v_m(r)=-4\pi(e/\lambda\!\!\!^{-}_{\mu})\int_0^r y^{-2}dy\int_0^y(F_m^2+G_m^2)dx, \tag{22}$$

assuming $F_m^2+G_m^2$ to be normalized as in the caption of Fig. 8. The change of the transition energies may then be expressed as single integrals over the change of charge density:

$$\Delta E_{m\to n}=\int_0^\infty S_{mn}(r)[\delta\rho(r)/Ze]4\pi r^2dr. \tag{23}$$

The quantity by which S_{mn} is multiplied in this expression is the fractional change of charge at the radius r; and S_{mn}, with the dimensions of energy, is given by

$$S_{mn}=-Ze(v_m-v_n). \tag{24}$$

Figure 9 shows the weighting functions S_{mn} for the $2P_{3/2}-1S$, the $3D\to2P_{3/2}$, the $3D\to2P_{1/2}$, and the $2S\to2P_{3/2}$ transitions. The normalized functions shown in Fig. 8 have been used to evaluate v_{1S}, v_{2S}, and v_{2P}; v_{3D} has been neglected in comparison with v_{2P}. For light nuclei, the weighting functions have the radial dependence: $S(2P\to1S)\sim-r^2$, $S(3D\to2P_{3/2})\sim-r^4$. For Pb, the peripheral charge is weighted relatively less in relation to the central charge than for light nuclei.

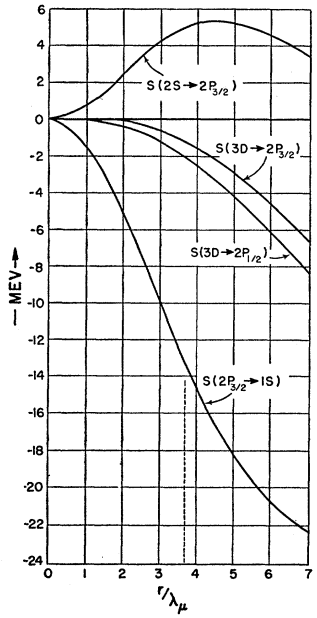

FIG. 9. The sensitivity of transition energies to distribution of nuclear charge is defined by the functions S_{mn} of Eqs. (22)–(24) and plotted here for four transitions. Entering into the calculation of S_{mn} are the expressions for μ-meson density

$$P_m(r)=4\pi(F_m^2+G_m^2).$$

When the normalized exact solutions for uniform nuclear charge were fitted to polynomials valid in the neighborhood of the nucleus, the results were, in terms of the dimensionless distance $\xi=r/\lambda\!\!\!^{-}_{\mu}$,

$$10^3P(1S)=140.71\xi^2+10.21\xi^3-24.91\xi^4+5.20\xi^5-0.32\xi^6,$$
$$10^3P(2P_{1/2})=6.565\xi^2+1.194\xi^3+3.657\xi^4-1.138\xi^5+0.086\xi^6,$$
$$10^3P(2P_{3/2})=3.423\xi^4+0.243\xi^5-0.537\xi^6+0.108\xi^7-0.007\xi^8,$$
$$10^3P(2S)=72.34\xi^2+3.12\xi^3-16.60\xi^4+3.97\xi^5-0.27\xi^6.$$

Inspection of Fig. 8 indicates that the above plotted sensitivities would not markedly change if derived for nuclear charge distributions other than uniform.

V. CONCLUSION

For light elements, the mu-mesonic transition energies determine only $\langle r^2\rangle_{Av}$ the average value of r^2 over the nuclear charge distribution.[5] This is the same quantity that is determined at low Z by most other effects sensitive to the extent of the nuclear charge distribution.

For heavy elements, the mu-mesonic spectrum is dependent upon the shape as well as the extent of the nuclear charge distribution. The present calculations for Pb serve two functions. (1) They provide predictions of the mu-meson spectrum for various charge distributions which may be compared with future, more precise, experiments on the mu-mesonic transition energies. The calculations, combined with other considerations on perturbations and uncertainties in the interpretation, indicate that the mu-mesonic transitions alone can provide a reasonable idea of the shape as well as the size of the nuclear charge distribution. (2) They limit the set of possible charge distributions which may be applied to the interpretation of other nuclear charge-sensitive experiments, if the value of the $2P\rightarrow 1S$ transition energy is used as a constraint. Some considerations of this use are given in the succeeding paper. More especially, these calculations should help in interpreting the high energy electron scattering experiments.[7] In order to test their utility in this regard, exact calculations of the scattering of very high energy electrons from the conceivable Pb nuclei considered here are now in progress.

The numerical results here reported were obtained with one of the Los Alamos I.B.M. Type 701 computers, in the use of which we have benefited from the experience of members of Los Alamos Group T-1, who have developed a number of standard programs employed in the present work.

Stimulating discussions with Professor John A. Wheeler of Princeton University contributed much to the initial formulation of these studies. We have profited also from conversations with Professor Rainwater and Dr. Cooper of Columbia University.

APPENDIX I. SOME INTEGRALS OVER THE ASSUMED CHARGE DISTRIBUTION

The normalization integral $I_f(\infty)$, defined by Eq. (6), and the dimensionless potential function $J_f(x)$, defined by Eq. (7), are here given for the various charge distribution functions, $f(x)$, defined in Part III.

Family I

$$I_f(\infty)=\tfrac{1}{3}(n+1)(n+2)(n+3),$$

$$J_f(x)=\frac{1}{x}(1-e^{-x})-e^{-x}\sum_{k=0}^{n} b_k\frac{x^k}{k!},$$

where

$$b_k=\frac{n+1}{n+2}-\frac{k}{k+1}-\frac{\tfrac{1}{2}n(n+1)-\tfrac{1}{2}(k-1)k}{(n+1)(n+2)(n+3)}.$$

Family IIa

$$I_f(\infty)=\frac{e^{-n}+2n+\frac{1}{3}n^3}{1-\frac{1}{2}e^{-n}};$$

$$J_f(x)=\left[1+\frac{1}{2}n^2-\frac{1}{6}x^2+e^{-n}\left(\frac{1-e^x}{x}+\frac{1}{2}e^x\right)\right]\Big/ \times(e^{-n}+2n+\tfrac{1}{3}n^3),\quad x<n;$$

$$J_f(x)=\frac{1}{x}-\frac{e^{n-x}[(1/x)+\frac{1}{2})]}{e^{-n}+2n+\frac{1}{3}n^3},\quad x>n.$$

Family IIb

$$I_f(\infty)=e^{-n}+2n+\tfrac{1}{3}n^3/n^3(1-\tfrac{1}{2}e^{-n}),$$

$$J_f(x)=\left[\frac{1}{n^2}+\frac{1}{2}-\frac{1}{6}x^2+\frac{e^{-n}}{n^2}\left(\frac{1-e^{nx}}{nx}+\frac{1}{2}e^{nx}\right)\right]\Big/ \left(\frac{1}{3}+\frac{2}{n^2}+\frac{e^{-n}}{n^3}\right),\quad x<1;$$

$$J_f(x)=\frac{1}{x}-e^{n-nx}\left(\frac{1}{x}+\frac{n}{2}\right)\Big/(e^{-n}+2n+\tfrac{1}{3}n^3),\quad x>1.$$

Family III

$$I_f(\infty)=\frac{1}{1-\frac{1}{2}e^{-n}}\left[\frac{s\cosh s-\sinh s}{s^3}+\frac{(n^2-s^2)s\cosh s+(n^2+s^2)\sinh s}{s(n^2-s^2)^2}+\frac{ne^{-n}}{(n^2-s^2)^2}\right],$$

$$J_f(x)=\frac{1}{D}\left\{\frac{n^2}{s^2(n^2-s^2)}\cosh s+\frac{ne^{-n}}{(n^2-s^2)^2}\frac{1}{x}-\frac{\sinh sx}{s^3x}+\frac{e^{-n}}{2s(n^2-s^2)^2}\frac{e^{nx}}{x}[(n^2+s^2)\sinh sx-2ns\cosh sx]\right\},\quad x<1;$$

$$J_f(x)=\frac{1}{x}-\frac{e^n}{2(n^2-s^2)^2s}\frac{e^{-nx}}{x}\cdot\frac{1}{D}[2ns\cosh sx+(n^2+s^2)\sinh sx],\quad x>1;$$

where

$$D=(1-\tfrac{1}{2}e^{-n})I_f(\infty).$$

Family IV

A. *Exponential:*

$$I_f(\infty)=2,$$

$$J_f(x)=\frac{1}{x}-e^{-x}\left(\frac{1}{x}+\frac{1}{2}\right).$$

B. *Modified Exponential:*

$$I_f(\infty)=8,$$

$$J_f(x)=\frac{1}{x}-e^{-x}\left[\frac{1}{x}+\frac{5}{8}+\frac{x}{8}\right].$$

C. *Gaussian:*

$$I_f(\infty)=\tfrac{1}{4}\sqrt{\pi},$$

$$J_f(x)=\frac{1}{x}\cdot\frac{2}{\sqrt{\pi}}\int_0^x \exp(-z^2)dz=\frac{1}{x}\operatorname{erf}x.$$

D. *Modified Gaussian:*

$$I_f(\infty)=\tfrac{5}{8}\sqrt{\pi},$$

$$J_f(x)=\frac{1}{x}\operatorname{erf}x-\frac{2}{5\sqrt{\pi}}\exp(-x^2).$$

E. *Square (uniform):*

$$I_f(\infty)=\tfrac{1}{3},$$

$$J_f(x)=1/x, \quad x>1,$$

$$J_f(x)=\tfrac{3}{2}-\tfrac{1}{2}x^2, \quad x<1.$$

APPENDIX II. REMARKS ON NUMERICAL METHOD

A Runge-Kutta method of integration is used to solve Eqs. (10), with a constant interval size of two-tenths of the meson reduced Compton wavelength, $\lambda\!\!\!^{-}_{\mu}$, or about (1/19) of the "correct" nuclear radius, as defined for the uniform charge model, except very close to the origin, where the first four intervals are $\frac{1}{16}$, $\frac{1}{8}$, $\frac{1}{4}$, and $\frac{1}{2}$ of the normal interval. The integrations are begun at $r=\lambda\!\!\!^{-}_{\mu}/80$ with the asymptotic solutions of Eq. (10):

$$\left.\begin{aligned} G&=Ax^{k+1},\\ F&=\frac{2k+1}{\gamma(1+\epsilon)+\alpha ZJ_f(0)}Ax^k,\end{aligned}\right\} \qquad k>0;$$

$$\left.\begin{aligned} G&=Bx^{-k},\\ F&=-\frac{\alpha ZJ_f(0)+\gamma(\epsilon-1)}{-2k+1}Bx^{-k+1},\end{aligned}\right\} \qquad k<0.$$

Here A and B are arbitrary constants. Each trial solution is extended to whatever radius is required to determine whether the trial eigenvalue is too high or too low. If the initial values of G are taken positive for the $1S$ and $2P$ states and negative for the $2S$ state, common criteria for high or low ϵ may be applied to all four states: (a) if G exceeds a previously chosen large number, $G_{\max}$, or if dG/dr passes from negative to positive while $G>0$, then ϵ is too small (binding energy too large); (b) if G passes fron positive to negative, then ϵ is too large. The initial trial binding energy for the $1S$ state was one-half of the central potential. The initial trial binding energy for the $2S$ and $2P$ states was one-half of the binding energy of the $1S$ state. Trial solutions were repeated for each assumed size and shape until the apparent eigenvalues had converged to one part in $2^{17}\cong 1.2\times 10^5$. Some experimentation with interval size indicated that for the interval above described the accuracy of the eigenvalues was also one part in 10^5.

For each shape of charge distribution, a number of values of the range parameter γ were used which led to $2P_{3/2}\rightarrow 1S$ energies of 6.00 Mev$\pm$20 percent. The initial value of γ was chosen such that the distribution in question had a mean value of r^2 approximately equal to that previously found for the uniform distribution.[4,5] Succeeding values of γ were chosen automatically by the machine, and a final value of γ was chosen by interpolating parabolically among the previous values for that range which would yield a $2P_{3/2}\rightarrow 1S$ energy of 6.00 Mev. The final energies calculated with this interpolated γ and the earlier interpolated energies agreed to about 1 kev, so that parabolic interpolation among the values of Table IV may be carried out with high accuracy.

The sequence of calculations was made automatic throughout the sizes and shapes of interest within each family. Listings are available of the potentials, and of the wave functions for the "correct" range, of each shape. Each line of Table IV represents about five minutes of automatic calculation.